
1

MICRO- AND NANO-STRUCTURED INTERPENETRATING POLYMER NETWORKS: STATE OF THE ART, NEW CHALLENGES, AND OPPORTUNITIES

JOSE JAMES¹, GEORGE V. THOMAS¹, AKHINA H.² AND SABU THOMAS^{2,3}

¹*Research and Post-Graduate Department of Chemistry, St. Joseph's College, Moolamattom, Kerala, India*

²*International and Interuniversity Centre for Nanoscience and Nanotechnology, Mahatma Gandhi University, Kottayam, Kerala, India*

³*School of Chemical Sciences, Mahatma Gandhi University, Kottayam, Kerala, India*

1.1 INTRODUCTION

Polymer mixtures are materials that play a significant role in modern industry. The preparation and properties of multicomponent polymeric systems are of great practical and academic interest. They provide a convenient route for the modifications of properties to meet specific needs. Interpenetrating polymer networks (IPNs) are one of the most rapidly growing areas in polymer material science. The golden history of IPN had begun with its discovery by Aylsworth in 1914 [1].

Micro- and Nano-structured Interpenetrating Polymer Networks: From Design to Applications, First Edition. Edited by Sabu Thomas, Daniel Grande, Uroš Cvelbar, K.V.S.N. Raju, Ramanuj Narayan, Selvin P. Thomas and Akhina H.

© 2016 John Wiley & Sons, Inc. Published 2016 by John Wiley & Sons, Inc.

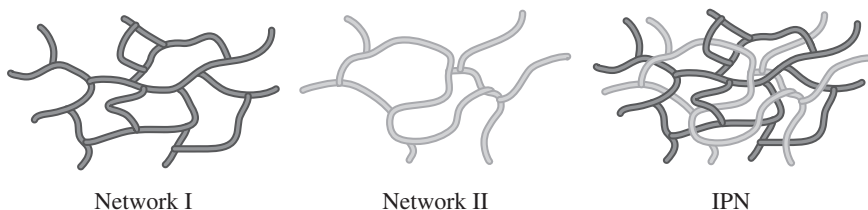


FIGURE 1.1 Schematic representation of component networks and IPN. Source: Klempler *et al.* [3]. Reproduced with permission of the American Chemical Society

IUPAC Compendium of chemical terminology defines IPNs as polymers comprising two or more networks that are at least partially interlaced on a molecular scale but not covalently bonded to each other and cannot be separated unless chemical bonds are broken [1, 2]. IPNs are a combination of incompatible polymer networks, at least one of which is synthesized and/or crosslinked in the presence of the other [3, 4] (Figure 1.1).

Figure 1.2 shows a schematic representation of mechanical blends, graft copolymers, block copolymers, semi-IPNs, and full-IPNs.

IPNs are in fact a special class of polymer blends. The two characteristic features of IPNs that distinguishes itself from the other types of multiphase polymer systems are as follows: (1) IPNs swell but do not dissolve in solvents and (2) creep and flow are suppressed in IPNs [5].

While the science of IPNs began with the work of Millar in 1960 [6], the first publication on the subject came through a patent by Aylsworth in 1914 [1]. Since then, IPNs have been the subject of extensive study by investigators looking into the synthesis, morphology, properties, and applications of these materials. Table 1.1 summarizes the history of IPNs and related materials [7, 8].

1.2 TYPES OF INTERPENETRATING POLYMER NETWORKS

Figure 1.3 classifies the following types of IPNs [1, 9]: semi-IPN, sequential IPN, simultaneous IPN, and full-IPN. They are grouped based on chemical bonding and rearrangement pattern.

1.2.1 Full-Interpenetrating Polymer Networks

They comprise two or more polymer networks, which are at least partially interlocked on a molecular scale but not covalently bonded to each other and cannot be separated unless chemical bonds are broken. It can be represented as in Figure 1.4a.

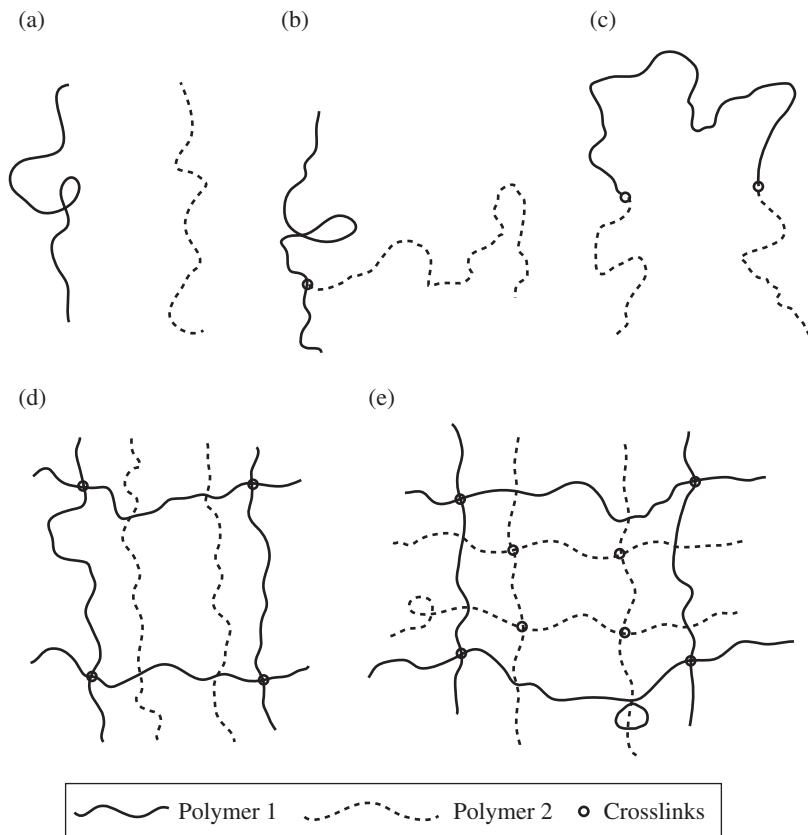


FIGURE 1.2 Schematic representation of (a) mechanical blends, (b) graft copolymers, (c) block copolymers, (d) semi-IPNs, and (e) full-IPNs. Source: Sperling and Mishra [5]. Reproduced with permission of John Wiley & Sons

TABLE 1.1 History of IPN

Year	Event	First Investigators
1914	IPN-type structure	J. W. Aylsworth
1927	Graft copolymers	I. Ostromislensky
1951	IPNs	J. J. Staudinger and H. M. Hutchinson
1952	Block copolymers	A. S. Dunn and H. W. Melville
1960	Homo-IPNs	J. R. Millar
1969	Sequential IPNs	L. H. Sperling
1969	Latex IPNs	K. C. Frisch, D. Klemptner, and H. L. Frisch
1971	Simultaneous IPNs	L. H. Sperling and R. R. Arnts
1974	IPN nomenclature	L. H. Sperling
1977	Thermoplastic IPNs	S. Davison and W. P. Gergen

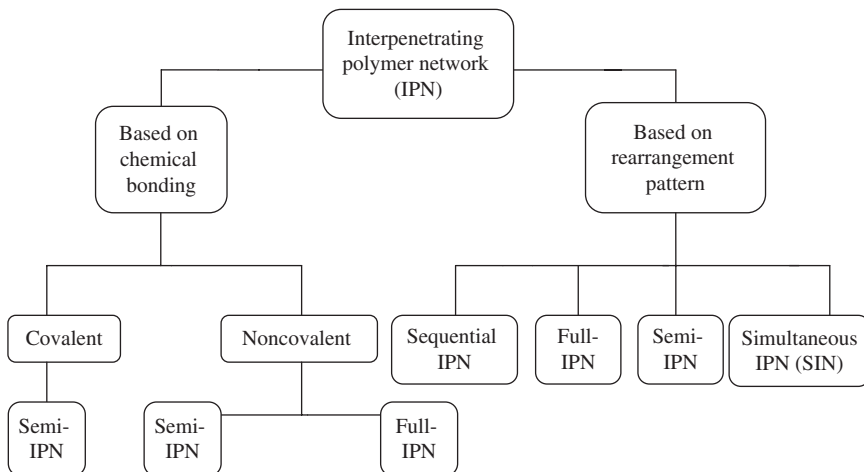


FIGURE 1.3 Classifications of IPNs. Source: Shivashankar, <http://www.ijppsjournal.com/>. Used under CC-BY-4.0 <http://creativecommons.org/licenses/by/4.0/>

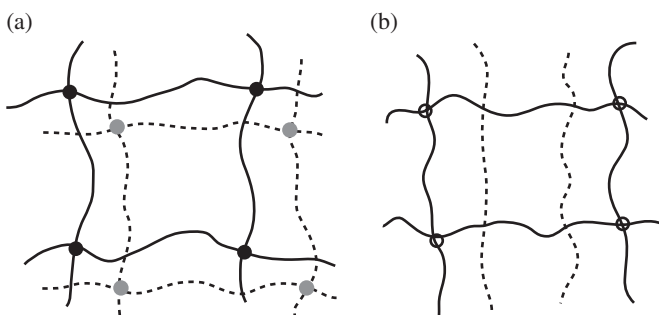


FIGURE 1.4 (a) Full-IPN. (b) Semi-IPN. Source: Sperling and Mishra [6]. Reproduced with permission of Taylor & Francis

1.2.2 Sequential Interpenetrating Polymer Networks

This type of IPN involves the preparation of a polymer network I followed by the *in situ* polymerization of monomer II along with crosslinker and activator, which are then swollen into the network I.

1.2.3 Simultaneous Interpenetrating Networks

In simultaneous interpenetrating networks (SINs), the monomers along with the crosslinkers and activators of both networks are mixed. The reactions are carried out simultaneously; however, they are noninterfering types of reactions such as chain and step polymerization reactions.

1.2.4 Latex Interpenetrating Polymer Networks

These IPNs are made in the form of lattices, frequently with a core and shell structure.

1.2.5 Gradient Interpenetrating Polymer Networks

Gradient IPNs are materials in which the overall composition or crosslink density of the material varies from location to location on the macroscopic level. For example, a film can be made with network I predominantly on one surface, network II on the other surface, and a gradient in composition throughout the interior.

1.2.6 Thermoplastic Interpenetrating Polymer Networks

Thermoplastic IPN materials are hybrids between polymer blends and IPNs that involve physical crosslinks rather than chemical crosslinks. Thus, these materials flow at elevated temperatures, similar to the thermoplastic elastomers, and at use temperature, they are crosslinked and behave like IPNs.

1.2.7 Semi-Interpenetrating Polymer Networks

In semi-IPNs, only one component of the assembly is crosslinked leaving the other in linear form. They are also called pseudo-IPNs. It can be depicted as in Figure 1.4b.

Mishra and Sperling [6] investigated semi-IPNs composed of poly(ethylene terephthalate) and castor oil. They found that bond interchange between these two materials played a major role in initial miscibility and morphology. The semi-IPNs displayed much better mechanical properties than the individual component materials did.

1.3 SYNTHESIS OF INTERPENETRATING POLYMER NETWORKS

The IPN synthesis techniques can be summarized as follows.

1.3.1 Sequential Interpenetrating Polymer Networks

This technique involves the sequential addition of selective crosslinkers to a homogenous mixture of two polymers in solution or in melt form [6]. They are in fact synthesized by a two-step process. In the first step, polymerization

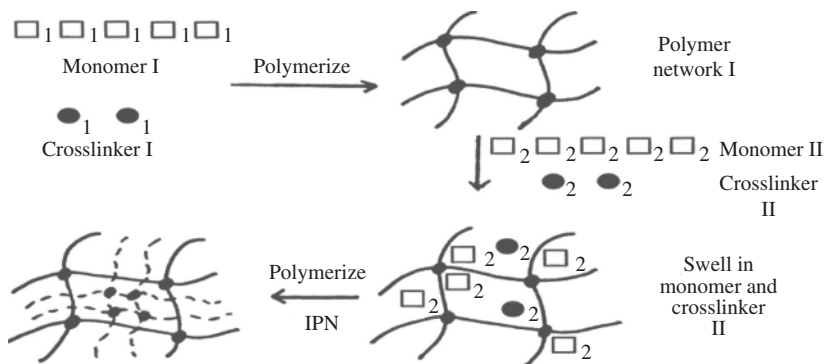


FIGURE 1.5 Schematic representation of sequential IPN synthesis. Source: Sperling [1]. Reproduced with permission of Springer

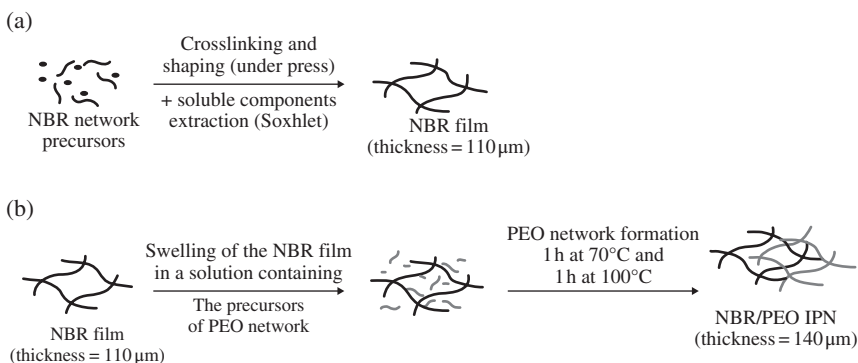


FIGURE 1.6 Outline of NBR/PEO IPN synthesis. (a) NBR network synthesis and (b) PEO network synthesis within NBR network. Source: Goujon *et al.* [10]. Reprinted with permission of the American Chemical Society

of first mixture (consisting of monomer, crosslinking agent, and initiator or catalyst) forms a network I. This network is swollen with the second combination of monomer and crosslinking agent and polymerized to form an IPN, that is, the polymer-2 is polymerized and crosslinked *in situ* in network I [6]. The route can be represented as in Figure 1.5.

Nitrile butadiene rubber/poly(ethylene oxide) (NBR/PEO) IPNs prepared by Goujon *et al.* successfully employed the sequential route for IPN synthesis [10]. Here, IPNs were prepared from NBR and PEO using a two-step process. The NBR network was obtained by dicumyl peroxide crosslinking at high temperature and pressure. A free radical copolymerization of poly(ethylene glycol) methacrylate and dimethacrylate led to the formation of the PEO network within the NBR network. It can be depicted as in Figure 1.6.

Sequential IPNs based on a nitrile–phenolic blend and poly(alkyl methacrylate) were prepared and characterized by Samui *et al.* [11]. The IPNs were not fully compatible but exhibited higher tensile strength compared to corresponding nitrile–phenolic blends. The strength increased with the increase in the concentration of poly(alkyl methacrylate).

1.3.2 Simultaneous Interpenetrating Networks

In SINs, a polymer is synthesized (from the monomer) and simultaneously crosslinked within the network of another polymer to give rise to an interpenetrating network [12]. Here, an IPN is formed by polymerizing two different monomers and crosslinking agent pairs together in one step. The key to the success of this process is that the two components must polymerize by reactions that will not interfere with one another. This is often accomplished by polymerizing one network by a condensation reaction, while the other network is formed by a free radical reaction. The route can be represented as in Figure 1.7.

A notable IPN synthesis by adopting sequential method was reported by M. Ivankovic *et al.* [13]. Here, IPN consists of methyl methacrylate (MMA) and an organically modified silicon alkoxide, 3-glycidyl oxy propyltrimethoxysilane (GLYMO), with varying MMA/GLYMO molar ratios.

SINs were first reported by Frisch by blending a urethane prepolymer with a low-molecular-weight epoxy resin [7]. In SINs, the relative rates of formation of each network would be the controlling factor in determining the morphology. It was also observed that the morphology of IPNs was slightly finer than the corresponding pseudo-IPN [8].

Classical works on IPN include damping applications [14], photodiodes from IPN [15], IPN membranes [16], complex-forming IPNs [17], fire-retarding IPNs [18], conducting IPNs [19], encapsulating IPNs, conducting hydrogel IPNs [20], elastomeric IPNs [21], and polymer solar cell based on IPNs [22].

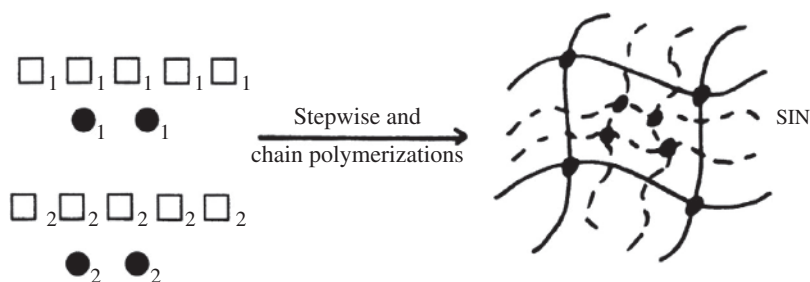


FIGURE 1.7 Schematic representation of simultaneous IPN synthesis. Source: Sperling *et al.* [1]. Reproduced with permission of Springer

1.4 CHARACTERIZATION OF INTERPENETRATING POLYMER NETWORKS

Modern instrumental techniques are used to characterize the interpenetration and ultimate properties of IPNs. Various methods are there to determine the morphology, thermal properties, physical properties, and other characteristics of IPNs. The interpenetration in IPN may be identified by:

1. Comparing the shift of dynamic glass transition temperatures of IPNs with their homopolymers.
2. Comparing the morphologies (micro- or nanoscale) and distribution of phase domains, shape, and sizes.

The existence of interpenetration is generally better judged through the combination of aforementioned inferences [23].

1.4.1 Morphology

The morphology of IPNs depends on the method of synthesis, on the compatibility of the polymer systems employed, and on the relative rates of formation. In sequential IPNs, the network first formed is most likely to be the continuous network. Its crosslink density is the controlling factor in determining the morphology of the system of each network [24]. The morphological properties of IPNs are best characterized by using the scanning electron microscopy (SEM) and transmission electron microscopy (TEM).

The micrographs obtained using the SEM and TEM appears to be useful in detecting the interpenetration of phase domains, shape, and structures of the order of magnitude of a micron to a tenth of a micron and the degree of mixing [25].

TEM is another powerful technique for the elucidation of IPN architecture. TEM analysis proves the fine distribution of PEO phase in continuous NBR phase for the IPN of the PEO–NBR system [10] (Figure 1.8).

Here, the black domains correspond to NBR-rich phases, and the white domains represent the PEO-rich phases. Since the TEM pictures are grayish, the boundary between the dark and clear gray regions is not obvious. This reinforces the fact that the IPN architecture is a very finely distributed PEO phase in a continuous NBR matrix.

A recent work on magnetically doped multistimuli-responsive hydrogel microspheres with IPN structure reported by Ahmad *et al.* [26] successfully employed SEM and TEM images for morphology characterization. In this

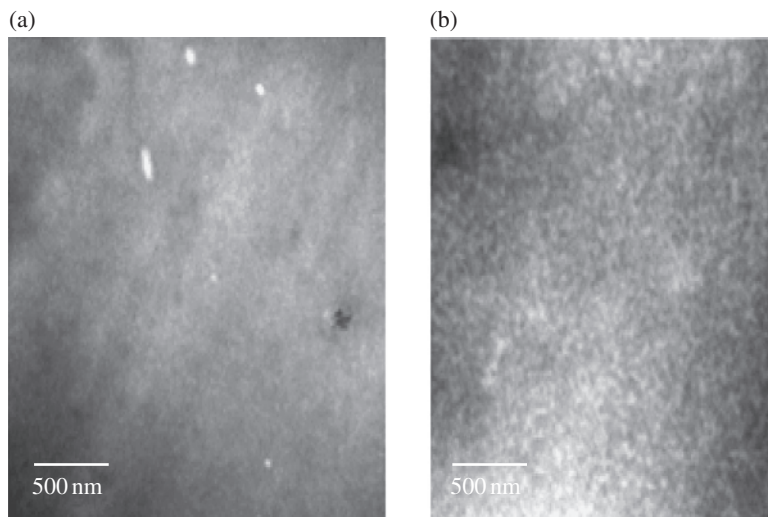


FIGURE 1.8 TEM pictures of NBR/PEO (50% PEGDM) IPN. Source: Goujon *et al.* [10]. Reprinted with permission of the American Chemical Society

study, it is found that the presence of Fe_3O_4 nanoparticles on the surface of P(NIPAM-MBAM)/P(MAA-EGDM) IPN hydrogel microspheres is clearly observed from microscope images. Both TEM and SEM images suggest that the deposition of Fe_3O_4 nanoparticles on the surface of P(NIPAM-MBAM)/P(MAA-EGDM) IPN hydrogel microspheres most likely improved the stability during sample preparation as the microspheres remained mostly spherical (Figures 1.9 and 1.10).

IPN based on polyisoprene and PMMA by John *et al.* [27] also employed SEM images as a powerful tool for characterization. SEM images of IPN (poly isoprene–PMMA IPN) at different compositions are given in the succeeding text. These are SEM images of IPNs with same crosslink density and varying compositions.

Figure 1.11a shows the sample with 20 wt% PMMA. It has a sea-island morphology. Figure 1.11b shows the sample with 35% PMMA. It shows a discrete state with larger domain dimension. In Figure 1.11c, the 50% PMMA composition shows a dual-phase morphology with polyisoprene as the matrix. The sample with 60% PMMA composition shown in Figure 1.11d shows a continuous phase morphology.

An unusual semi-IPN nanoencapsulating layer composed of thermally cured polyimide (PI) and polyvinyl pyrrolidone (PVP) with lithium cathode materials (here LiCoO_2 (LCO)) reported by Kim *et al.* utilized the potential application of SEM and TEM images for morphology characterization [29]. The surface

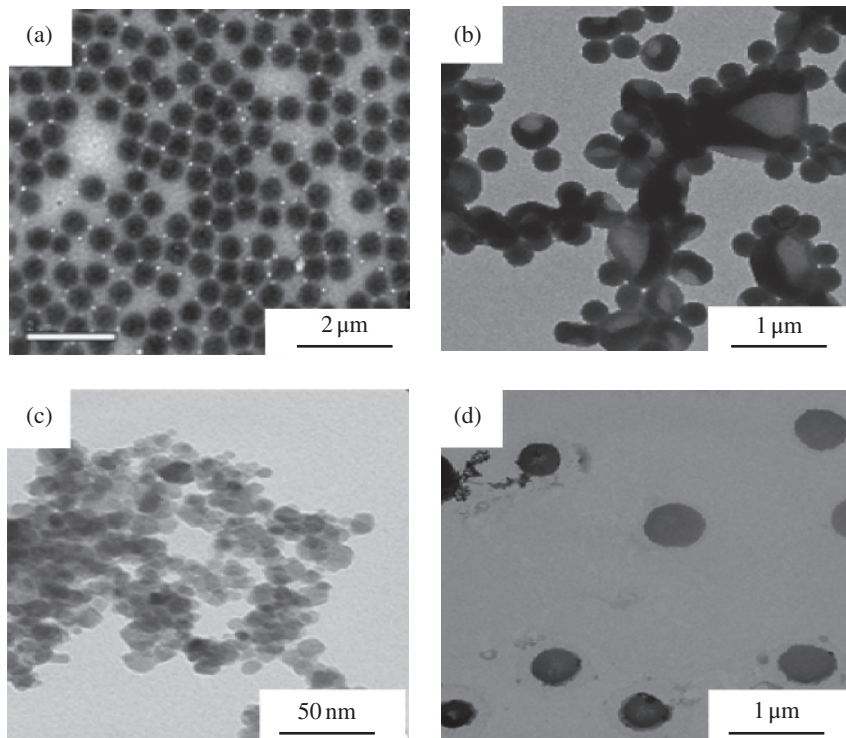


FIGURE 1.9 TEM images of (a) P(NIPAM-MBAM) hydrogel microspheres, (b) P(NIPAM-MBAM)/P(MAA-EGDM) IPN hydrogel microspheres, (c) Fe_3O_4 particles, and (d) P(NIPAM-MBAM)/P(MAA-EGDM)/ Fe_3O_4 IPN hydrogel microspheres. Source: Ahmad *et al.* [26]. Reprinted with permission of Elsevier

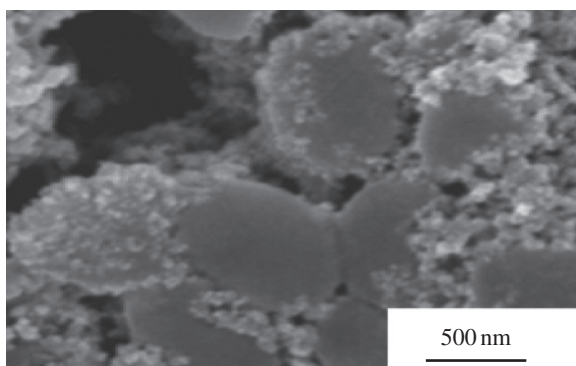


FIGURE 1.10 SEM image of washed P(NIPAM-MBAM)/P(MAA-EGDM)/ Fe_3O_4 IPN hydrogel microspheres. Source: Ahmad *et al.* [26]. Reprinted with permission of Elsevier

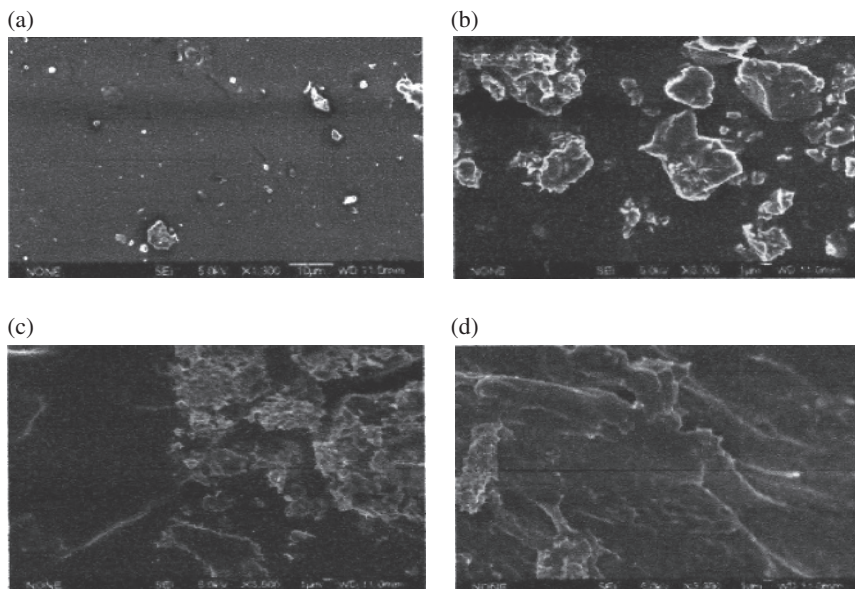


FIGURE 1.11 SEM images of PI-PMMA (a) with 20 wt% PMMA, (b) with 35% PMMA, (c) with 50% PMMA, and (d) with 60% PMMA. Source: John *et al.* [28]. Reproduced with permission of Elsevier

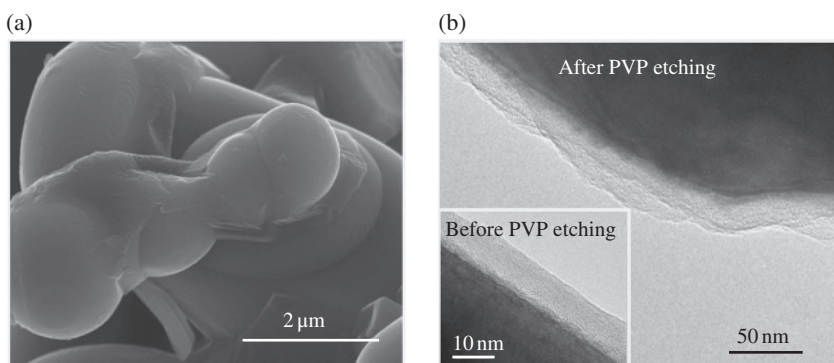


FIGURE 1.12 Structural characterization of PI/PVP-LCO. (a) FE-SEM photograph; (b) TEM photographs before/after selective etching of PVP phase. Source: Kim *et al.* [29]. Reproduced with permission of Nature Publishing Group

morphology of PI/PVP-LCO was characterized with a focus on coverage area of the LCO surface. Figure 1.12a shows that the PI/PVP-LCO has highly continuous and conformal polymeric layers on the LCO surface. The highly continuous conformal morphology of the PI/PVP nanoencapsulating layer was further elucidated by conducting TEM studies (Figure 1.12b).

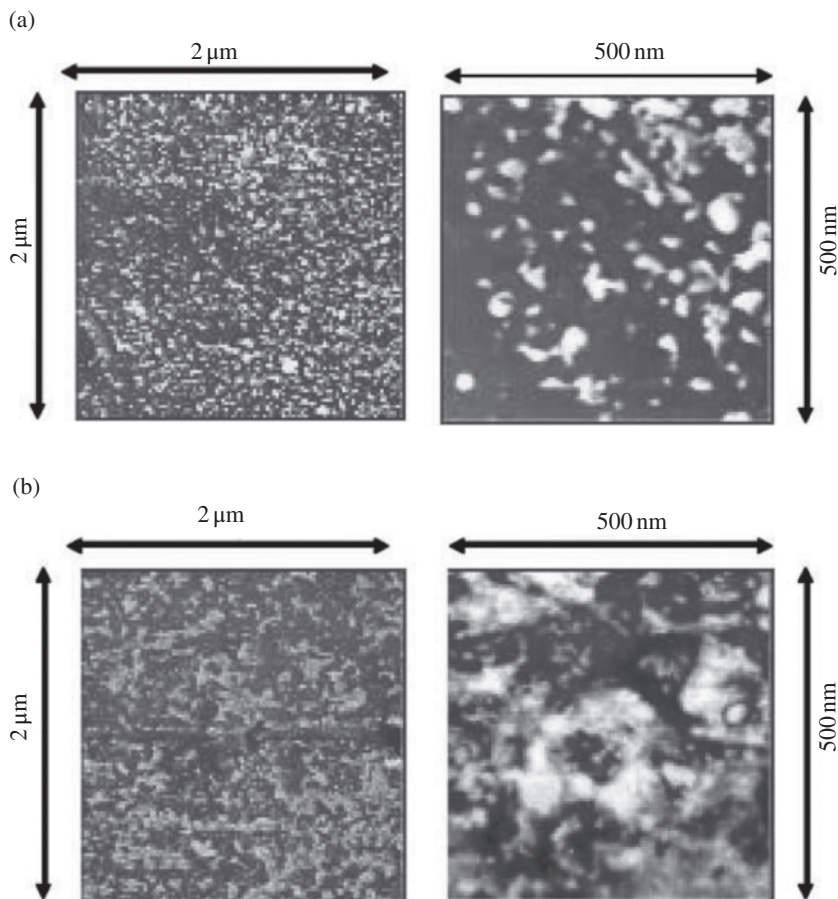


FIGURE 1.13 (a) AFM images of PIB/PMMA (60/40) IPN. (b) AFM images of PIB/PMMA (30/70) IPN. Source: Vancaeyzeele *et al.* [30], figures 6, 7. Reprinted with permission of Elsevier

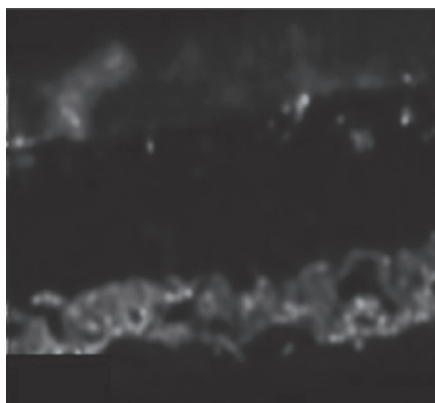
Atomic force microscopy (AFM) analysis also provides valuable information on the IPN morphology. It helps to differentiate continuous phase and dispersed phase in IPN. AFM is also used to identify the domain size of the components in IPN. In the characterization of polyisobutene (PIB)–PMMA IPN, AFM was used successfully to elucidate the morphology as shown in Figure 1.13a and b [30].

Confocal laser-scanning microscopy (CLSM) also provides some useful insight into IPN morphology [31]. It helps to identify the hydrophilic and hydrophobic regions of hydrogel type IPN. X-ray scattering experiments are widely used for enlightening the morphology of IPN [32]. It can be used for

(a)



(b)



(c)

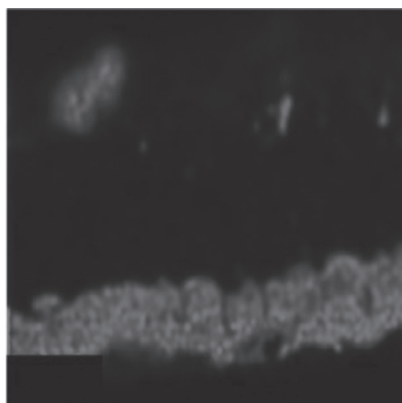


FIGURE 1.14 (a) SEM images of NBR-PEDOT network. (b) EDAX analysis showing the repartition of sulfur, (c) that of oxygen in the NBR-PEDOT semi-IPN. Source: Francke *et al.* [33]. Reprinted with permission of Elsevier

the visualization of interpenetrating channels in IPN. Energy-dispersive X-ray analysis (EDAX) explains the distribution of dispersed phase in the IPN matrix [33]. SEM pictures and EDAX analysis give immediate information about the repartition of polyethylenedioxythiophene (PEDOT) within the NBR matrix. The scanning electron micrograph of a cross section of NBR/PEDOT semi-IPN obtained at 10kV is shown in Figure 1.14a.

As expected, this picture clearly shows the formation of a heterogeneous system: the two different phases observed correspond to pure NBR (phase 1) and PEDOT/NBR (phase 2). We can deduce that PEDOT interpenetrates within the NBR matrix. This observation corroborates the fact that PEDOT cannot be

removed from the surface of the matrix by scratching. From the SEM picture, the depth of interpenetration can be estimated around $35\ \mu\text{m}$. Moreover, the distribution of the characteristic elements S and O of PEDOT in the cross-sectional area observed in the EDAX mapping (Figure 1.14b and c) clearly indicated that PEDOT was present inside the NBR in its doping state as expected.

Laser scanning confocal microscopy (LSCM) is a very good technique to provide the morphology of IPN as a function of depth [34].

1.4.2 Thermal Properties

The collective observations from electron microscopy and thermal measurements provide the real morphology of an IPN. Differential scanning calorimetry (DSC), thermogravimetric analysis (TGA), differential thermal analysis (DTA), and so on have been extensively used to study the thermal properties of IPN [35].

DSC shows one or two T_g values (shifted or unshifted) based on the extent of interaction between the components. The T_g s often lie at or between the T_g s of the pure networks. The appearance of single T_g indicates the formation of an IPN, and in this case, one can rule out the formation of any macro-/micro-phase separation. The slight shifting and broadening of the peaks indicate a moderate degree of molecular mixing [35]. In many cases, two distinct T_g s corresponding to those individual component networks have been observed. Such behavior has been reported by Sperling and others [36]. Merging of T_g s or an inward shift can be considered as evidence for the interpenetration of phases in IPN [37] (Figure 1.15).

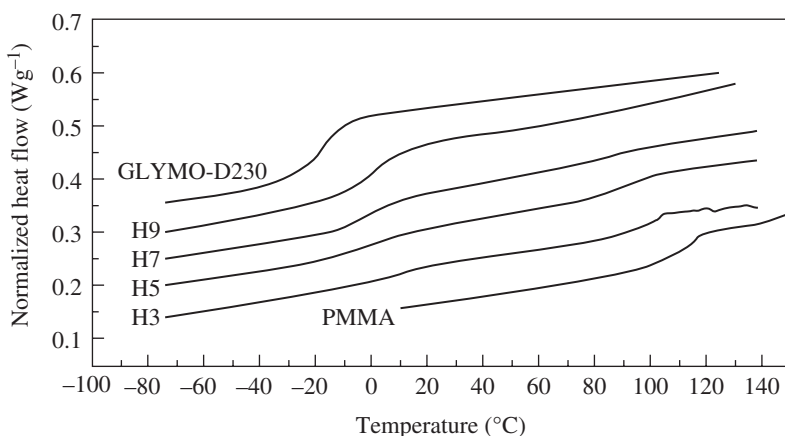


FIGURE 1.15 DSC thermograms of PMMA and hybrid systems. Source: Ivankovic *et al.* [13]. Reproduced with permission of Elsevier

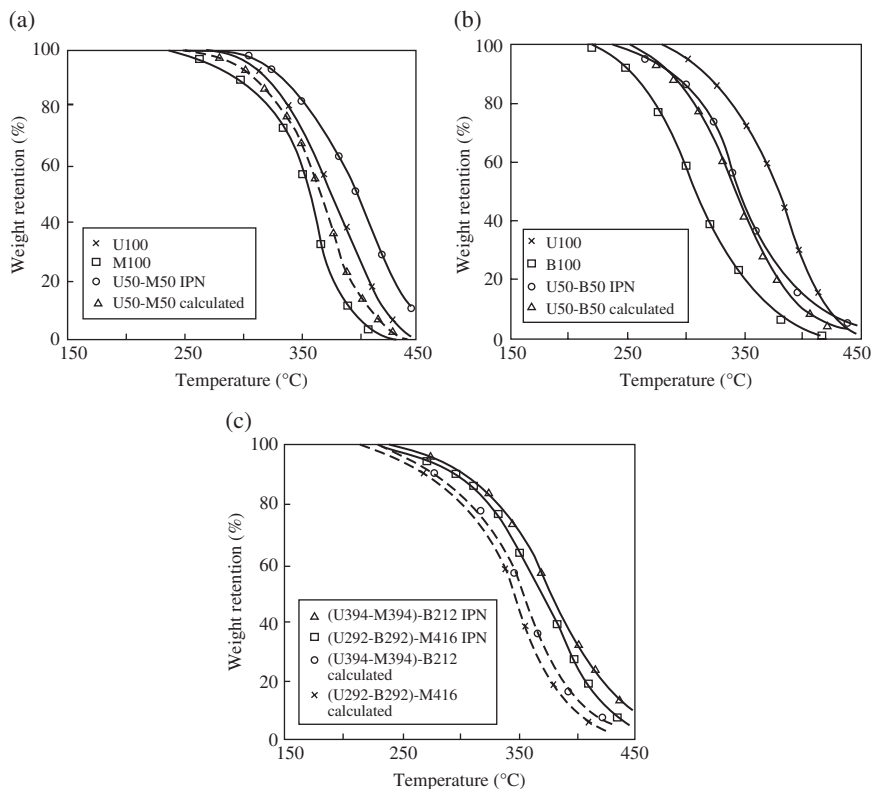


FIGURE 1.16 TGA thermograms of PU-PMMA SIN (a), PU-PBMA SIN (b), and three-component IPN homopolymers (c). Source: Lee and Kim [32]. Reproduced with permission of Nature Publishing Group

Ivankovic *et al.* [13] has used the DSC technique for the characterization of organic–inorganic hybrids based on PMMA and sol–gel-polymerized glycid-yloxypropyl trimethoxysilane (GLYMO). The glass-transition temperatures of the GLYMO and PMMA were -17 and 114°C , respectively. The hybrids showed two T_g values suggesting heterophase morphology.

The weight loss of IPNs indicates the thermal stability of IPNs. In most reports, the thermal stability of the IPN has been found to be higher than their homopolymers [38]. The enhancement or depression in thermal stability during IPN formation can be best explained in terms of TGA [39]. Thermal stability characteristics of three-component IPNs have been compared with two-component IPNs with the aid of TGA analysis by Lee and Kim [32].

By comparing Figure 1.16a and b, it can be concluded that PU-PMMA SIN possesses better thermal stability than PU-PBMA SIN. From Figure 1.16c, the enhanced thermal stability of three-component IPNs can also be understood.

1.4.3 Mechanical Properties

The composition and nature of the constituent polymeric network defines the mechanical properties of IPN. Common mechanical properties used to characterize IPN are tensile strength, elongation at break, Young's modulus, and hardness [39]. Mechanical properties (tensile stress–strain behavior, tensile stress relaxation, and tensile creep) were extensively used to elucidate the composition of IPN of the PEA–PMMA system [40]. From the following tensile stress relaxation master curves and dynamic mechanical properties (Figures 1.17 and 1.18), one can get the idea of kinetics of the formation of IPNs and the extent of interpenetration in sequential IPN of the PEA–PMMA system.

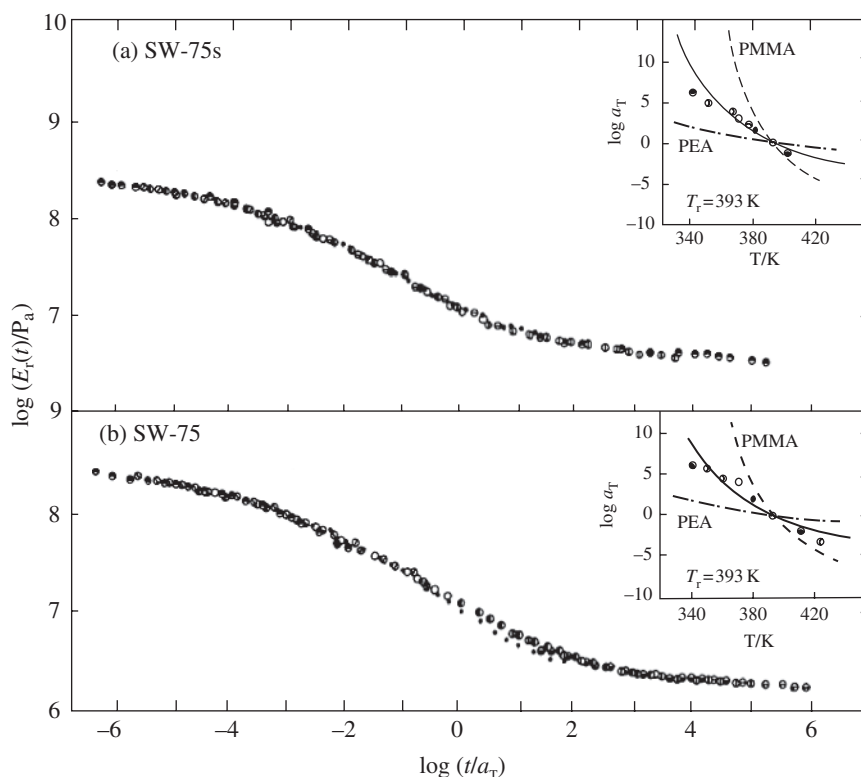


FIGURE 1.17 Tensile stress relaxation master curves for (a) semi-IPN and (b) full-IPN. Curves in the inset represent the WLF equation for PEA–PMMA and IPN. Source: Adachi and Kotaka [40]. Reproduced with permission of Nature Publishing Group

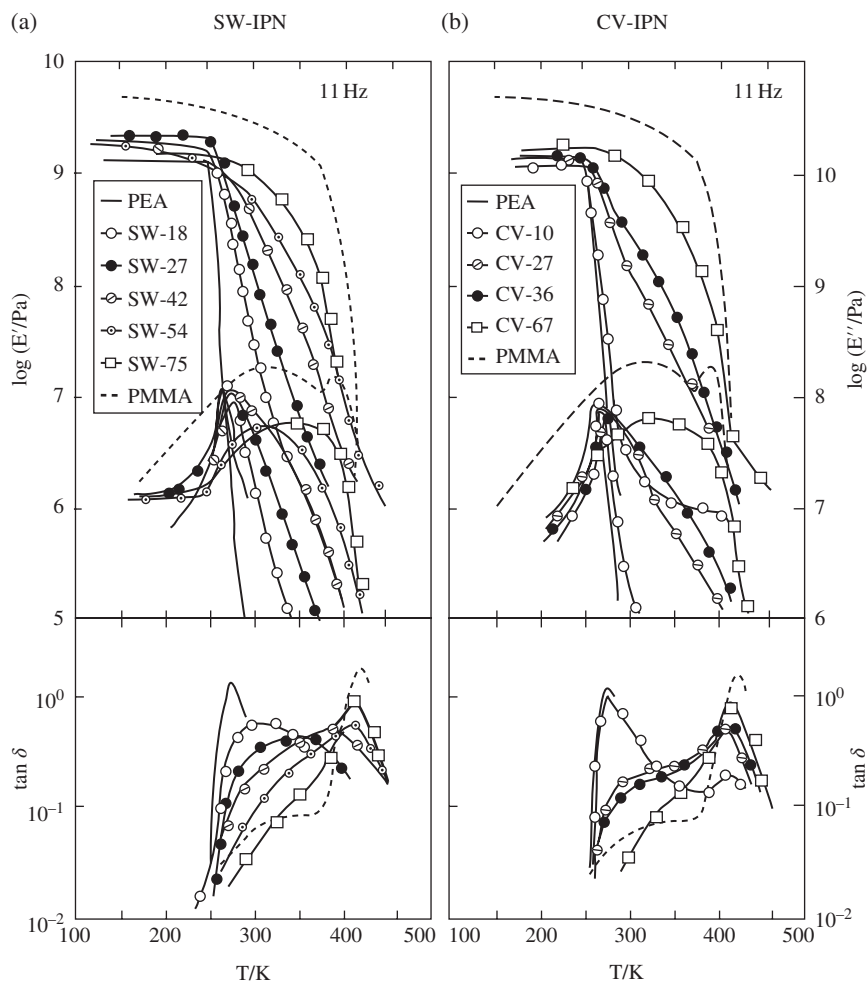


FIGURE 1.18 Storage (E') and loss (E'') modulus and loss strength ($\tan \delta$) plotted against temperature for (a) SW- and (b) CV-full-IPNs. CV, convert ion-controlled IPN; SW, swelling ratio-controlled IPN. Source: Adachi and Kotaka [40]. Reproduced with permission of Nature Publishing Group

1.4.4 Kinetic Properties

In an ideal IPN, the two components are present as co-continuous, interlocking networks. This co-continuity can be achieved by the kinetic retention of the initial mixture of the monomers used to form network chains, with phase segregation inhibited by the network structure. Gel time, solidification time, and crystallization time are used to represent the kinetic formation of IPNs from its constituent polymeric networks [39]. Rheological methods are used

to determine the gel point. The gel points at various temperatures can be used to calculate the activation energy of crosslinking. Kinetic results were used as a guideline to optimize the conditions of polymerization. Kinetic control and phase segregation are the chief controlling factors in the morphology of IPN.

1.4.5 Spectroscopic Techniques

The spectroscopic methods that are widely used in the structure elucidation are nuclear magnetic resonance (NMR), infrared (IR), and electron spin resonance (ESR) techniques. NMR spectroscopy is used to estimate the nanoscale interpenetration of polymers in IPN. The spin–lattice relaxation time measurements may also give some insight into the domain size [41]. Solid-state NMR has been proven a fruitful technique to investigate the microstructure and molecular dynamics of IPNs. Detailed information about morphology, miscibility, microstructure, and mobility can be directly accessed by NMR studies [39, 41]. The interaction between PMMA/NR (natural rubber) IPNs was analyzed using the C-13 relaxation measurements at room temperature by John *et al.* [28] (Figure 1.19).

The wide-line separation (WISE) NMR spectroscopy is used to measure the dynamics of solid polymers by correlating the proton line shape with

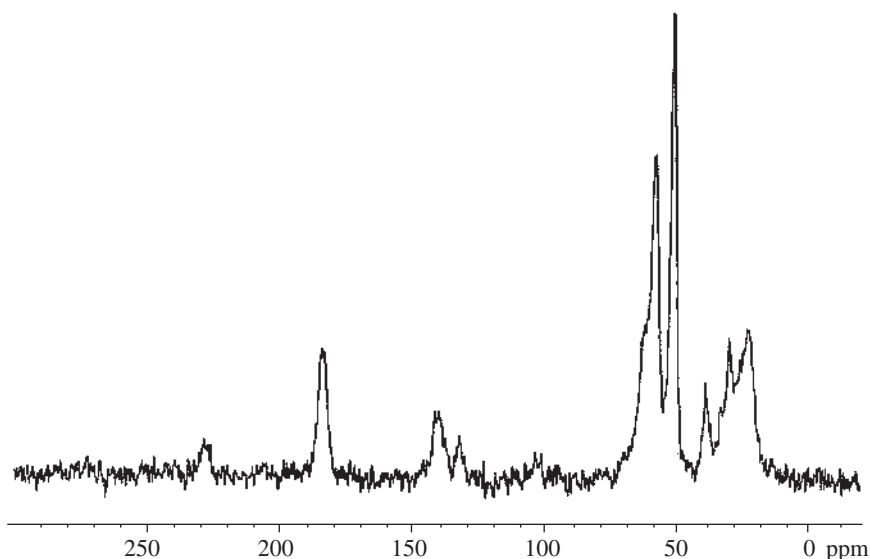


FIGURE 1.19 C-13 NMR spectrum of semi-IPN. Source: John *et al.* [28]. Reproduced with permission of Elsevier

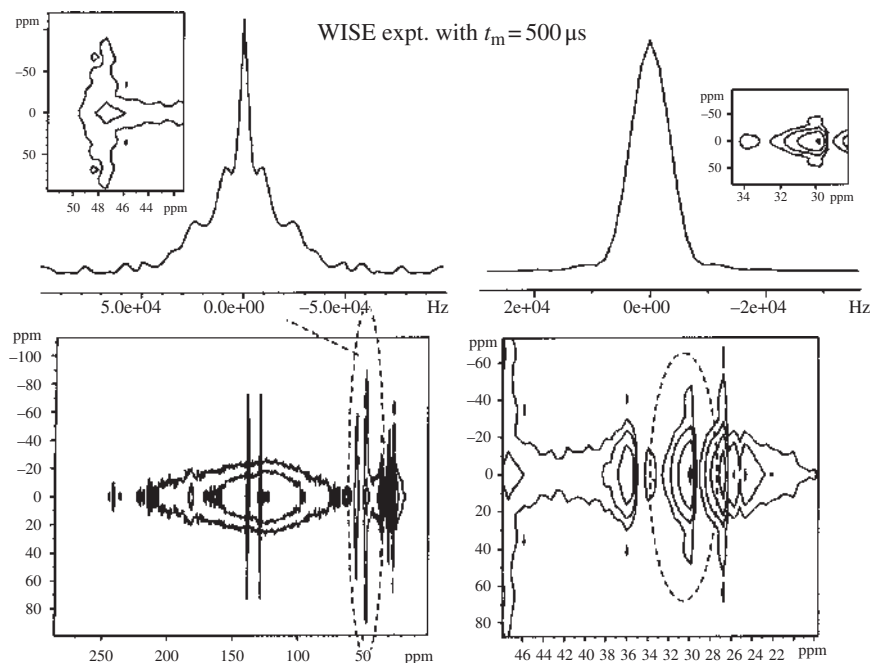


FIGURE 1.20 Contour plot of the WISE NMR spectrum of NR/PMMA semi-IPN. Source: John *et al.* [28]. Reproduced with permission of Elsevier

carbon chemical shift. This experiment yields information about dynamics by measuring the degree to which the proton line shapes are averaged by molecular motion. The WISE experiment does establish a correlation of the chemical structure and segmental mobility as reflected in the C-13 chemical shifts and the H-1 line shapes, respectively. Figure 1.20 shows contour plots of the WISE NMR spectrum of PI/PMMA 50/50 semi-IPN at 298 K [28].

Figure 1.20 shows contour plots of the WISE NMR spectrum of PI/PMMA 50/50 semi-IPN at 298 K. *Several well-resolved peaks are observed, including the PI proton peaks for $-\text{CH}_2-$ at 36 ppm, other $-\text{CH}_2-$ at 30 ppm, and $-\text{CH}-$ group at 129 ppm. From the PMMA phase, protons of the $-\text{CH}_2$ group at 50 ppm, $-\text{OCH}_3$ at 54 ppm, and $-\text{CH}_3$ at 27 ppm are clearly resolved. Peaks at 27 ppm contain overlapped peaks from methyl groups in PI and PMMA. The contour plot shows very different proton line widths for the PMMA and NR chains. This is the characteristic of a phase-separated multicomponent system consisting of rigid and mobile phases. The WISE experiment shows that the protons in the ester group (54 ppm) of PMMA have the highest mobility and $-\text{CH}_2-$ protons at 50 ppm are the most rigid among protons in the PMMA phase. 2D WISE experiment also showed the unusual high mobility in the*

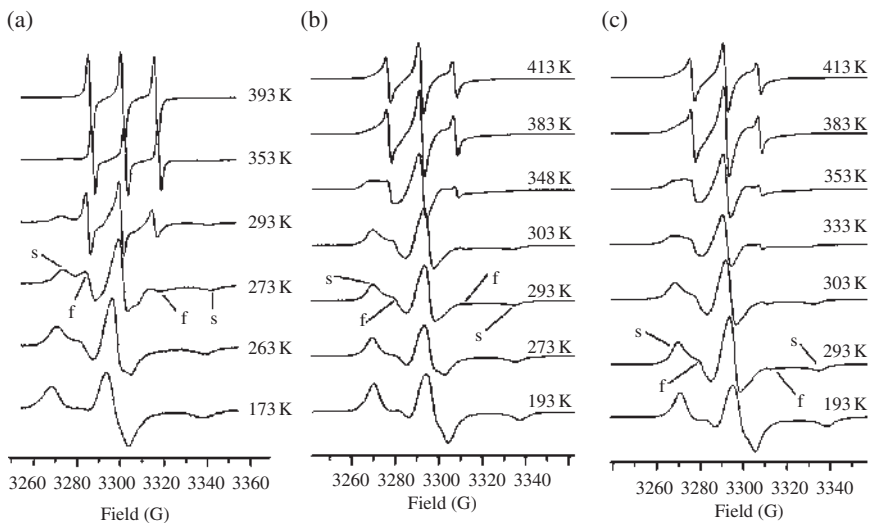


FIGURE 1.21 ESR spectra of probe measured as a function of temperature in (a) NR, (b) semi-IPN with 35 wt% of PMMA, and (c) semi-IPN with 50/50 composition. Source: John *et al.* [28]. Reproduced with permission of Elsevier

H atoms attached to the ester carbon of PMMA, proving the influence of highly flexible environment close to PMMA chains.

ESR spectroscopy is another technique used for the characterization of IPNs. ESR spectroscopy is widely used as a potential tool for the understanding of the structure and heterogeneities in IPN on a length scale that is less than 5 nm. ESR line shapes and spectral simulation data are used to arrive at some morphological conclusions along with the help of SEM and TEM. ESR spectra of the spin probes in semi-IPNs with different composition, crosslink density, and molecular weight were measured in the temperature range of 173–413 K at intervals of 10 K or less. ESR spectra of probe measured as a function of temperature for NR (poly isoprene) and for different semi-IPN of the NR-PMMA system [28] are shown in Figure 1.21. The free nitroxide radical 4-hydroxy-2,2,6,6-tetramethylpiperidine-1-oxyl was used as a spin probe for ESR measurements. In this study, the main conclusions from ESR investigations of PI-PMMA IPNs were as follows:

1. At lower temperatures, the ESR spectra approached the rigid limit spectrum and as the temperature increased, the spectral lines got narrowed and outer peaks shifted inward. In the range of 293–373 K, complex spectra were obtained, which is an indication of the presence of motionally distinct regions in semi-IPNs.

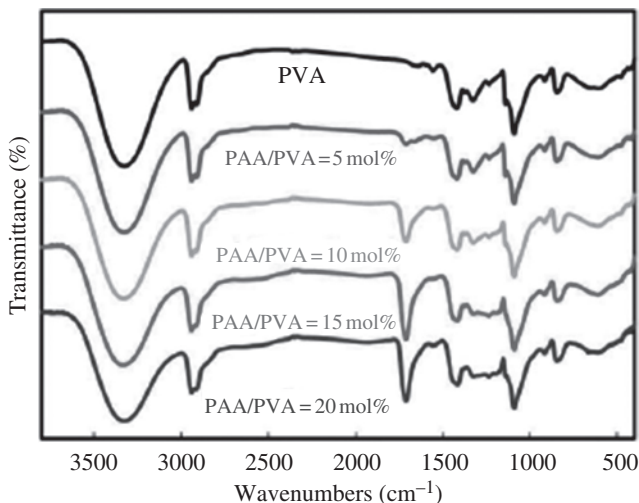


FIGURE 1.22 FT-IR spectrum of PVA-PAA IPNs. Source: Lu *et al.* [42]. Reproduced with permission of Elsevier

2. Semi-IPN synthesis resulted in a dramatic change in the motional behavior of both polymers, and this was due to the molecular level interpenetration between two polymer chains. The intimate mixing of the rigid PMMA chains with highly mobile NR networks strengthened the NR networks.

IR and FT-IR spectroscopic techniques have been widely used for identifying the components with their special groups in IPNs. This forms additional tools to confirm the completion of reaction and to diagnose the networks [42]. The FT-IR spectra of PVA/PAA IPN films with different PAA contents (0, 5, 10, 15, and 20 mol% of AA monomer per vinyl alcohol repeating unit) are shown in Figure 1.22.

The FT-IR spectrum of pure PVA hydrogel membrane shows the main characteristic bands as follows: 3300 cm^{-1} at the O—H stretching vibration, 2941 and 2910 cm^{-1} at the C—H stretching vibration, 1421 and 1328 cm^{-1} at the C—H deformation vibration, 1241 cm^{-1} at the C—O stretching vibration, 1090 cm^{-1} at the C—O stretching vibration, and 917 cm^{-1} at the O—H bend. With an increase of PAA content in IPN hydrogels, the C—O stretching band of PAA at 1711 cm^{-1} was boosted up and shifted gently toward the lower wave numbers, while the C—O stretching vibration of pure PVA at 1241 cm^{-1} was gradually enhanced and broadened. This indicates that new intermolecular hydrogen bond interaction in the IPNs was formed, which is in evidence that the hydrogen bond interactions of PVA hydrogel are replaced by hydrogen

bond interactions between PVA and PAA [42]. Moreover, the peak of the O—H stretching vibration for the pure PVA membrane, at 3300cm^{-1} , was gradually broadened and weakened, while the C—O stretching vibration at 1090cm^{-1} was slightly strengthened. This may be caused by the etherification reaction between carboxylic acid groups in PAA and hydroxyl groups in PVA. The study with the FT-IR spectra confirmed the formation of the PVA/PAA IPN hydrogel.

1.4.6 Viscoelastic Measurements of Interpenetrating Polymer Networks

This is one of the major tools for characterization of IPNs. Dynamic mechanical analysis (DMA) is widely used for the measurement of viscoelastic behavior of IPNs. DMA is a technique used to characterize IPN's properties as a function of temperature, time, frequency, stress, or a combination of these parameters. It measures stiffness and damping (dissipation of energy) in a material under cyclic loading. In DMA experiments, the SINs show either two well-defined glass transitions [43]. This may be due to three possibilities via gelation of polymer 1, gelation of polymer 2, and phase separation of polymer 1 from polymer 2.

Reddy and Takahara reported on the DMA of thermosensitive transparent semi-IPNs for wound dressing and cell adhesion control applications [44]. In this work, semi-IPNs were composed of segmented polyurethane urea/poly (*N*-isopropylacrylamide) (SPUU/PNiPAAm). Figure 1.23 shows the storage modulus (E') and loss modulus (E'') versus temperature of SPUU and semi-IPNs. The damping peak is associated with the partial loosening of the polymer structure so that small chain segments can move, which occurs near T_g at low frequencies. The maximum in the loss modulus (E'') at low frequencies is, however, very close to T_g (here T_g is -19°C). The increase in T_g observed due to addition of PNiPAAm could be attributed to the more interaction of PNiPAAm chains with SPUU soft segments. It is also observed from Figure 1.23 that the damping peak height decreases with the addition of PNiPAAm (curves 2–5).

Figure 1.23 also shows dynamic storage modulus (E') as a function of temperature. A sharp decrease of E' in the case of parent polymer above the glassy region has been observed. However, in the case of semi-IPNs, a systematic decrease of rubbery plateau region or high rubbery plateau modulus (E') has been observed with an increase of PNiPAAm content, which implies that elastic behavior predominates rather than rubbery behavior with PNiPAAm. This may be due to the increased number of interactions between SPUU and PNiPAAm.

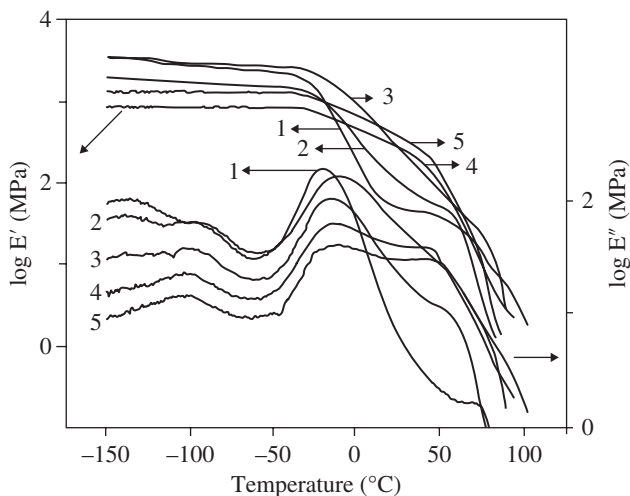


FIGURE 1.23 Dynamic mechanical analysis of SPUU and semi-IPNs: (1) NEAT SPPU, (2) SPPU with 20% PNiPAAm, (3) SPPU with 30% PNiPAAm, (4) SPPU with 40% PNiPAAm, and (5) SPPU with 50% PNiPAAm. Source: Reddy *et al.* [44]. Reproduced with permission of the American Chemical Society

1.5 APPLICATIONS OF INTERPENETRATING POLYMER NETWORKS

IPNs have variety of applications and they are in fact commercially successful form of polymer blends, probably owing to the crosslinked structure that provides better thermal stability, mechanical properties, chemical resistance, and so on [9]. IPNs are traditionally used as damping materials, impact-resistant materials, adhesives, and so on. The immense applications of IPNs are summarized in the following chart. Their unique properties of specificity, mechanical strength, swelling capacity, nutrient and oxygen permeability, durability in the body, and sensitivity can be identified [9] (Table 1.2).

1.6 FUTURE TRENDS

Recently, IPNs are combined with nanoparticles to produce high-performance nanocomposites. IPN-supported scaffold [45] is one of the growing area of polymer blends. Nanocomposite polymer IPN hydrogels are new-generation materials useful for a wide variety of applications [46]. They are used as responsive hydrogels [44, 46–48], medical implants, porous scaffolds [49] or

TABLE 1.2 Potential Applications of IPN [9, 10, 23]

Components	Application
Natural leather/rubber	Improved leather
Plastic/rubber	Noise damping, tough plastic
Plastic/plastic	Optically smooth surfaces
Rubber/rubber	Pressure-sensitive adhesives
Rubber/plastic	Impact modifier
Rubber/crystalline plastic	Thermoplastic, elastomer
Rubber/water-swellaable phase	Arteriovenous shunt
Xanthan gum/PVA	IPN microsphere
Grafted Na alginate/Na alginate	IPN-based tablets
Poly acrylamide/PVA	IPN hydrogel capsule
Collagen/glycosaminoglycan	IPN-based sponges for wound dressing
PGA/collagen (3D scaffold)	Bioengineering tissue
Collagen/hydroxyapatite	Bone substitute
Collagen/chitosan	Cartilage scaffold
PMMA/poly(butyl acrylate)	Noise damping coating
PMMA/PMMA	Dental filling

catalyst supports, self-healing materials, thermosensitive materials, contact lenses [50], and so on. The new applications of IPN are controlled drug delivery systems [51], energy storage materials [48], corneal transplantation [52], and use in fuel cells [48]. IPNs have immense scope in tissue engineering and as an uteral stents [50]. Thus IPN holds many advancements and future applications that will be of immense help to mankind. The literature survey of latest works on IPN reveals that current thrust areas of IPN are hydrogel [47, 51, 53], polymer solar cell [22], controlled drug release [54, 55], and thermo-sensitive IPN for wound dressing [44]. IPN hydrogels are called hungry networks or intelligent polymers due to their potential technological application in medicine, industry, biology, and environmental cleanup [56].

One of the shining future aspects of IPN is in the manufacture of solar cell [57]. Here, incoming photon from the sun creates exciton (electron hole pair) that travels to interface where charge separation occurs, producing useful voltage. IPN has found immense use in various biomedical applications [58] and in biochemistry [59]. IPN electrolyte is another thrust area in the polymer research field [60].

The outlook for IPNs is exceedingly bright and is a hot research area. The data from ISI web of science indicate that China, United States, and India are the leaders in IPN research area, and currently about 500 papers per year are being published in this research field. Processing techniques for the synthesis of eco-friendly IPNs and clear differentiation of physical and chemical

interpenetration using characterization techniques are the still remaining gaps in this field. Despite many advances, numerous challenges and opportunities remain for making an impact in the field of smart interpenetrating polymers.

ACKNOWLEDGEMENT

Financial support from Council of Scientific and Industrial Research is duly acknowledged.

REFERENCES

- [1] Sperling, L.H. (1981) *Interpenetrating Polymer Networks and Related Materials*, Plenum Press, New York, pp. 1–30.
- [2] Donatelli, A.A., Sperling, L.H. and Thomas, D.A. (1981) *Macromolecules*, **15**, 625.
- [3] Klempner, D., Sperling, L.H. and Utracki, L.A. (1994) *Interpenetrating Polymer Networks*, American Chemical Society, Washington, DC, pp. 39–75.
- [4] Aylsworth, J.W. (1914) Plastic Composition. US Patent 1,111,284A.
- [5] Sperling, L.H. and Mishra, V. (1996) *Polymers for Advanced Technologies*, **7**, 197.
- [6] Mishra, V. and Sperling, L.H. (1996) *The Polymeric Materials Encyclopedia: Synthesis, Properties, and Applications*, CRC Press, Boca Raton.
- [7] Mathew, A.P. (2013) *Advances in Elastomers I*, Springer Verlag, Berlin/Heidelberg, pp. 282–300.
- [8] Mathew, A.P. (1999) Interpenetrating polymer networks based on natural rubber and poly styrene. Ph.D. thesis. Mahatma Gandhi University.
- [9] Shivashankar, M. and Mandal, B.K. (2012) *International Journal of Pharmacy and Pharmaceutical Sciences*, **4**, 1–7.
- [10] Goujon, L.J., Khaldi, A., Maziz, A. *et al.* (2011) *Macromolecules*, **44**, 9683–9691.
- [11] Samui, A.B., Suryavanshi, U.G., PatriI, M. *et al.* (1998) *Journal of Applied Polymer Science*, **68**, 255–262.
- [12] Mathew, A.P., Packrisamy, S., Kumaran, M.G. and Thomas, S. (1995) *Polymer*, **36**, 4935–4942.
- [13] Ivankovic, M., Brnardic, I. and Gajovic, A. (2009) *Polymer*, **50**, 2544–2550.
- [14] El-Aasser, M.S., Hu, R., Dimonie, V.L. and Sperling, L.H. (1999) *Journal of Colloids and Interfaces*, **153**, 241–253.
- [15] Halls, J.J.M., Walsh, C.A., Greenham, N.C. *et al.* (1995) *Nature*, **376**, 498–500.
- [16] Lee, Y.K., Sohn, I.S., Jeon, E.J. and Kim, S.C. (1991) *Polymer Journal*, **23** (5), 427–433.

- [17] Nishi, S. and Kotaka, T. (1989) *Polymer*, **21** (5), 393–402.
- [18] Chiu, H.T., Chiu, S.H., Jeng, R.E. and Chung, J.S. (2000) *Polymer Degradation and Stability*, **70**, 505–514.
- [19] Gan, L.H., Gan, Y.Y. and Yin, W.S. (1999) *Polymer*, **40**, 4035–4039.
- [20] Lu, Y., He, W., Cao, T., *et al.* (2014) *Scientific Reports* **4**, 1–8, article number: 5792.
- [21] Xie, H.Q. and Guo, J.S. (2002) *European Polymer Journal*, **38**, 2271–2277.
- [22] Ma, W. and Heeger, A.J. (2005) *Advanced Functional Materials*, **15**, 1617–1622.
- [23] Anandaraj, T., Mohan, P.S., Krishnan, S.M. and Raghavan, M. (2001) *Paintindia*, **4**, 43–54.
- [24] Das, B. and Gangopadhyay, T. (1992) *European Polymer Journal*, **8**, 867.
- [25] Thomas, S., Visakh, P.M., Chandra, A.K. and Mathew, A.P. (2013) *Advances in Elastomers II: Blends and IPNs*, Springer, Berlin.
- [26] Ahmad, H., Nurunnab, M., Rahman, M.M. *et al.* (2014) *Colloids and Surfaces A: Physicochemical and Engineering Aspects*, **459**, 39–47.
- [27] John, J., Suriyakala, R., Thomas, S. *et al.* (2010) *Journal of Materials Science*, **45**, 2892–2901.
- [28] John, J., Klepac, D., Didovi, M. *et al.* (2010) *Polymer*, **51**, 2390–2402.
- [29] Kim, J.M., Park, J.H., Lee, C.K. and Lee, S.Y. (2014) *Scientific Reports*, **4**, 4602.
- [30] Vancaeyzeele, C., Fichet, O., Laskar, J. *et al.* (2005) *Polymer*, **46**, 6888–6896.
- [31] Jones, D.S., Andrews, G.P., Caldwell, D.L. *et al.* (2012) *European Journal of Pharmaceutics and Biopharmaceutics*, **82**, 563–571.
- [32] Lee, J.H. and Kim, S.C. (1984) *Polymer*, **16** (6), 453–459.
- [33] Francke, I.F., HenriAubert, P., Alfonsi, S. *et al.* (2012) *Solar Energy Materials & Solar Cells*, **99**, 109–115.
- [34] Turner, J.S. and Cheng, Y.L. (2003) *Macromolecules*, **36**, 1962–1966.
- [35] Hou, S.S. and Kuo, P.L. (2001) *Polymer*, **42**, 9505–9511.
- [36] Donatelli, A.A., Sperling, L.H. and Thomas, D.A. (1976) *Macromolecules*, **9**, 676.
- [37] Yeo, J.K., Sperling, L.H. and Thomas, D.A. (1982) *Polymer Engineering & Science*, **22**, 190.
- [38] Thomas, S., Chandra, A.P. and Visakh, P.M. (2012) *Advances in Elastomers I: Blends and Interpenetrating Networks*, Springer, Berlin, pp. 1–70.
- [39] Pfeifer, C.S., Shelton, Z.R., Szczpanski, C.R., Barros, M.D., Wilson, N.D. and Stansbury, J.W. (2014) *Journal of Polymer Science, Part A: Polymer Chemistry*, **52**, 1796–1806.
- [40] Adachi, H. and Kotaka, T. (1982) *Polymer*, **14** (5), 379–390.
- [41] Parizel, N., Meyer, G. and Weill, G. (1995) *Polymer*, **36** (12), 2323–2330.
- [42] Lu, Y., Wang, D., Li, T. *et al.* (2009) *Journal of Biomaterials*, **30**, 4143–4151.

- [43] Sperling, L.H. (2003) *Encyclopedia of Polymer Science and Technology*, vol. **10**, John Wiley & Sons, New York, pp. 272–311.
- [44] Reddy, T.T., Kano, A., Maruyama, A., Hadano, M. and Takahara, A. (2008) *Journal of Biomacromolecules*, **9**, 1313–1321.
- [45] Botero, A.J., Blanco, M., Li, Y.Y., McGunnies, G. and Goodard, W.A. (2010) *Journal of Computational and Theoretical Nanoscience*, **7**, 1238–1256.
- [46] Therian, H. and Kumacheva, E. (2013) *Journal of the American Chemical Society*, **135**, 4834–4839.
- [47] Thankam, F.G., Muthu, J., Sankar, V. and Gopal, R.K. (2013) *Journal of Colloids and Surfaces B: Biointerfaces*, **107**, 137–145.
- [48] Noel, V. and Randriamahazaka, H.N. (2012) *Journal of Electrochemistry Communications*, **19**, 32–35.
- [49] Aduba, D.C., Jr, Hammer, J.A., Yuan, Q. *et al.* (2013) *Journal of Acta Biomaterialia*, **9**, 6576–6584.
- [50] Venkatesan, N., Shroff, S., Jayachandran, K. and Doble, M. (2010) *Journal of Endourology*, **4**, 191–198.
- [51] Huang, Y., Liu, M., Chen, J., Gao, C., Gong, Q. and Huang, Y. (2012) *European Polymer Journal*, **48**, 1734–1744.
- [52] Zhang, Q., Fang, Z., Cao, Y. *et al.* (2012) *ACS Macro Letters*, **1**, 876–881.
- [53] Murthy, P.S.K., Murali Mohan, Y., Varaprasada, K. *et al.* (2008) *Journal of Colloid and Interface Science*, **318**, 217–224.
- [54] Rani, M. and Negi, Y.S. (2010) *African Journal of Pharmacy and Pharmacology*, **4** (2), 35–54.
- [55] Anirudhan, T.S. and Parvathy, J. (2014) *International Journal of Biological Macromolecules*, **67**, 238–245.
- [56] Shidhaye, S., Surve, C., Dhone, A. and Budhkar, T. (2013) *International Journal of Research and Reviews in Pharmacy and Applied Science*, **2**, 637–650.
- [57] Jiang, B., Pu, H., Pana, H., Changa, Z. and Jina, M. (2014) *Journal of Electrochimica Acta*, **132**, 457–464.
- [58] Zhao, N. and Liu, S. (2011) *European Polymer Journal*, **47**, 1654–1663.
- [59] Liu, X.D., Kubo, T., Diao, H.Y., Benjamas, J., Yonemichi, T. and Nishi, N. (2009) *Journal of Analytical Biochemistry*, **393**, 67–72.
- [60] Bar, N. and Basak, P. (2014) *The Journal of Physical Chemistry C*, **118**, 10640–10650.

